2.4 GHz and 5.2 GHz Frequency Bands Reconfigurable Fractal Antenna for Wearable Devices using ANN

Sivabalan Ambigapathy [1] and Jothilakshmi Paramasivam [2*]

[1] Department of Electronics and Communication Engineering
Chennai Institute of Technology, Chennai, Tamil Nadu – 600 069, India
sivabalana@citchennai.net

[2] Department of Electronics and Communication Engineering
Sri Venkateswara College of Engineering, Chennai, Tamil Nadu – 602 117, India
jothi@svce.ac.in*

Abstract ─ Patch antenna is being used widely in wearable and implantable devices due to its lightweight characteristics. Multi-band patch antenna designs are possible by incorporating professional naturally inspired fractal pattern generating methodologies. Automated Frequency Characteristics Analyzer (AFCA), Artificial Neural Network based Fractal Pattern Generator (AFPG) and Nitinol based Pattern Selector (NPS) functional modules are proposed in this work to design a Dual band Reconfigurable Fractal Antenna for Wearable Devices (DRFA). Producing a miniature fractal patch antenna to support famed 2.4 GHz and 5.2 GHz frequency bands with lesser than 20db return loss is the objective of this work. Numerous fractal patterns are generated with the help of AFPG and their frequency responses are analyzed by Ansys HFSS (High Frequency Structure Simulator) through AFCA module. The results are provided to the AFPG part to train the neural network with proper biasing updates. The fitness function is set to the dimension restriction of 3000 square μm with less than 20 return loss at commonly used 2.4 GHz and 5.2 GHz. The feed type and length of the patches are also fine-tuned by the proposed AFPG module.

Index Terms ─ Artificial neural network, dual band antenna, fractal patterns, patch antenna, reconfigurable antenna, wearable device.

I. INTRODUCTION

Communication gadgets are getting tinier every so often. A range of these gadgets comes under the wearable communication sensor devices, which are involved hugely in health monitoring systems and remote patient monitoring systems. More than 761million people will be at their age 65 by 2025 [1] supposed to be overseen by the E-Health monitoring system. It requires an extensive number of wearable devices to be connected eventually under one or more networks. These devices frequently required to communicate with a centralized organizer to produce cumulative impact assessments. Sometimes they need to communicate directly with a network facility. These hypothetical situations require the support for multiband or reconfigurable communication facility. Leading communication technologies require 2.4 GHz for local Wi-Fi communications and 5.2 GHz for direct internet connectivity.

Lightweight, small size, sufficient gain and harmless flexible construction material are the presumed characteristics of a reconfigurable antenna for wearable devices [2]. Designing Antenna in the patch format is a known solution to achieve these characteristics. Selection of the shape and the dimension of the patch is a challenging work. The complexity of utilizing high cost multilayer Printed Circuit Board (PCB) can be avoided by selecting a suitable resonating antenna pattern in patch antenna design [3]. Microstrip patch antenna manufacturing is very economic while comparing conventional PCB based antenna designs.

Bandwidth enhancements are additional benefit of using microstrip patch antennas [4]. The frequency reconfigurable capability is achieved comfortably by selecting a suitable antenna pattern in microstrip patch antenna design [5]. Different approaches come into existence for optimizing antenna patterns such as Genetic Algorithm (GA) [6], Particle Swarm Optimization (PSO) [7], Bacterial Forage Optimization (BFO) [8] and Ant Colony Optimization (ACO) [9]. Blending one or more optimization algorithms or combining optimizations with ANN models are auxiliary approaches of finalizing an antenna pattern.

Recent studies show that the fractal patterns are used to devise astonishing antennas with multiband support [10, 11]. This work is indented to apply ANN to generate multiple fractal patterns based on a triangular structure mounted on different wearable substrates with different thickness to achieve an antenna pattern that supports 2.4

Submitted On: June 22, 2020
Accepted On: October 20, 2020
https://doi.org/10.47037/2020.ACES.J.360315

and 5.2 GHz. The bandwidth, return loss and gain of the generated fractal pattern antenna are evaluated along with similar existing antennas.

II. EXISTING WORKS

A compact dual band metamaterial antenna with $42 \times 32mm^2$ dimension is established in Dual Band Metamaterial Antenna for LTE / Bluetooth / WiMAX system (DMAL) work [12]. A Square metallic stripe is placedin such a way to cover the patch for lower band support. Similar magnetic current loop is provided near the feed to support upper band. The supporting frequency bands of this antenna are 0.6 ~ 0.64 GHz, 2.67 ~ 3.4 GHz and 3.61 ~ 3.67 GHz. Basic antenna designing principles are used to bring out the antenna patch pattern manually. There is no automatic optimizations are used to trim the pattern in this work. The authors used CST (Computer Simulation Technology) Microwave Studio Simulator to simulate the patch antenna pattern. The design is also fabricated for analyzing the frequency characteristics in real-time. The fabricated antenna is observed for 0.5 GHz to 4 GHz in Satimo StarLab – which can handle the frequency of up to 18 GHz. The gain and return loss graphs are provided to indicate that there is no significant difference between the simulated and observed results.

There are two different antenna designs are introduced in Integrated Dual-band Filtering/duplexing Antennas (IDFA) work [13]. The first design uses Coupled Resonator Technique to design a Dual-band Dual-polarization (DBDP) antenna. Each polarization has two bands obtained by placing a vertical hairpin resonator coupling with the patch. Both the bands show second order filtering performance and improved bandwidths. Dual-port dual-band antenna with integrated filtering and duplexing functionalities is introduced as the second antenna design. Two sets of resonator-based filtering channels are used to carry out the frequency duplexing functionality. The performance of the proposed antennas is measured in terms of gain and S-Parameters. The DBDP antenna resonates with 4.75 ~ 4.98 GHz band and 5.75 ~ 6.05 GHZ frequency bands. A good isolation index of less than 30 dB is achieved by the first design pattern. Two transmission voids are introduced between 4.8 and 5.85 GHz by cross coupling the resonators on purpose. These transmission voids are used to improve the isolation between the two polarizations.

A high gain Dual-polarized Dual-band Antenna (DDA) is designed in this work to support 2G, 3G and LTE indoor communication [14]. Two horizontal polarization and one vertical polarization elements are used to achieve the requirement. The upper horizontal polarization element is designed with four pairs of altered printed magneto-electric dipoles with four-way power divider feeding network. Eight pieces of arc shaped parasitic patches are printed on circular shaped printed circuit board. The lower horizontal polarization element is designed very similar to the upper horizontal polarization element except the parasitic patches. The four-way power divider feeding network enables a persistent radiation in $360°$ with high gain. The vertical polarization element is designed with 4-pairs of cone-shaped patches. Ansys HFSS is used to simulate the entire antenna pattern and a prototype is fabricated for real-time analysis. Based on the results, it is realized that the simulated and observed results are comparable to each other except some observation glitches.

This work Low-profile Dial-band Stacked Microstrip Monopolar Patch Antenna (LDSMMPA) is about to bring up a by coupling annular ring with conductive passages in the antenna structure [15]. The height of this antenna is set to be 4.175 mm. The utilization scope of this antenna is wireless local area network which operates in 2.4 to 2.48GHz and 5.75 to 5.825 GHz. Car-to-Car Communication networks with 5.85 to 5.925 GHz is another prime beneficial utilization of this antenna. The stacked-patch assembly of LDSMMPA is given in Fig. 1. A coaxial feed that connects directly to the center of the upper circular patch. The lower circular patch is fed by a coupling between interior probe and the lower circular with the clearance hole. This feeding arrangement enables better isolation between the two patches, so that the antenna can resonate at two frequency bands exquisitely. Ansys HFSS is used to simulate the antenna pattern and Agilent E5080A near filed measurement system is used to measure the frequency characteristics of the pattern. Both simulation and implementation results are in coherence, displays that the gain of 6 dBi is achieved for 2.24 ~ 2.53 GHz lower frequency band and the gain of 7.5 dBi is achieved for 5.42 ~ 5.98 GHz higher frequency band.

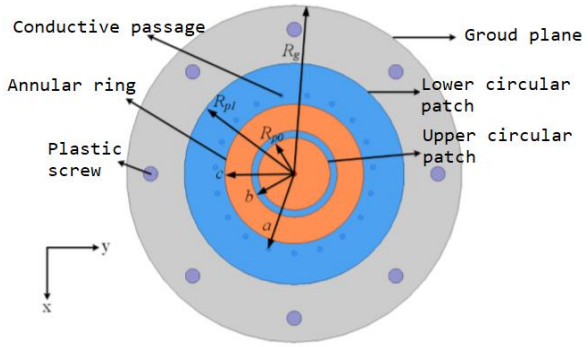

Fig. 1. Stacked-patch assembly.

A novel dual band hexagonal antenna for bluetooth and UWB applications with single band notched is indented to create a broadband antenna that supports 2.2 GHz ~ 2.52 GHz and 3.5 GHz to 10 GHz without interfering the WLAN frequency band 5.72 GHz ~ 5.825 GHz [16]. The core idea behind this work is to design an antenna that supports Bluetooth frequency and UWB

frequency bands without meddling WLAN frequency band. A circularly polarized dual-port dual-band RFID antenna that operates in UHF and UWB frequency bands is aimed in this work [17]. An adequate quadruple feed network in hybrid mode is used to achieve the wide frequency band resonance from 0.918 GHz ~ 0.926 GHz UHF band to 3.1 GHz ~ 4.8 GHz UWB band.

Miniature dual-band antennas are the major requirement in the multipurpose digital gadget world. Many communication devices are equipped with more than one communication facility such as GSM, LTE, Bluetooth and IEEE 802.11 b/g/n standards. Providing separate Antenna for every communication system will increase the size of the device significantly. Two widely used frequencies in these portable electronic communication devices are 2.4 GHz and 5 GHz. Manually designing a suitable dual-band antenna by checking various shapes and materials one-by-one will consume more time.

III. RELATED WORKS

There are two related works tracked down to the proposed DRFA work. They are Miniaturized Hexagonal-triangular Fractal Antenna for wide-band applications (MHFA) [18]and Novel Dualband Coaxial-fed SIW Cavity Resonator Antenna using ANN Modeling (NDCAANN) [19]. Certain salient points from these related works are discussed concisely in this section for better comprehension of the proposed DRFA method.

Fractal patterns are getting importance in antenna designing in recent times due to their multiband supporting characteristics. Generating fractal patterns is an amusing mathematical process which can develop multitudinous splendid effective patterns. There are several procedures introduced recently to create fractal patterns. In MHFA work, a hexagonal triangle fractal antenna design is proposed to get multiband resonating antenna between 3GHz ~ 25GHz. The size of the fractal antenna is restricted to $25mm \times 30mm$ with $0.8mm$ substrate thickness.

The following equation is used to find the resonant frequency of circular patch antenna:

$$f_\gamma = \frac{Ymn C}{5.714\, R_e \sqrt{\epsilon_{reff}}}, \quad (1)$$

where $Ymn = y_{11}$ for mode $TM_{11} = 1.8412$, $Ymn = y_{21}$ for mode $TM_{21} = 3.0542$, C refers the speed of light, ϵ_{reff} refers the effective dielectric constant, R_e refers the effective radius of the circular patch antenna.

R_e can be calculated using the following equation:

$$R_e = R_c \times \sqrt{\left(1 + \frac{2 \cdot t}{R_c \cdot \pi \cdot \epsilon_r} \times \left[\ln\left(\frac{\pi \cdot R_c}{2 \cdot t}\right) + 1.7726\right]\right)}, \quad (2)$$

where R_c refers the radius of circular patch antenna.

The value of f_γ hexagonal patch antenna can be calculated using the following equation:

$$f_\gamma = \pi \times (R_e)^2 = \frac{3}{2} \times \sqrt{3} \cdot S_h^2, \quad (3)$$

where S_h is the side length of the hexagonal patch antenna.

The effective dielectric constant ϵ_{reff} is calculated as:

$$\epsilon_{reff} = \frac{1+\epsilon_r}{2}. \quad (4)$$

The formation of hexagonal patch antenna over the circular shape is arranged with four 1mm hexagonal rings placed with a 2.5mm separation distance. Symmetrical triangular slots are used in the rear side of the hexagonal patch antenna to provide the channel insulation properly. This antenna achieved less than 20dB return loss in center frequencies 8GHz, 11GHz, 16GHz and 24GHz makes it eligible to use in 3GHz~25GHz bands.

Substrate Integrated Waveguide (SIW) is one of the most resent methodologies in generating compact low-loss comprehensive systems. SIW cavity resonators are widely used most modern antennas that supports millimeter and microwave devices. The dimensions involved in designing SIW cavity antenna is a strategically challenging task. This challenging task can be handoff to the computers with the help of machine learning computer aided tuning methods. There are several cover the counter machine learning algorithms exist such as Linear Regression, Logistic Regression, Decision Tree, Support Vector Machines and Random Forest.

ANN is a simple straight forward method used in many machine learning applications. NDCAANN takes advantage of this method to fine-tune the antenna pattern with computer aided tuning. The resonant frequency of the SIW cavity antenna can be calculated based on dimension of the SIW cavity using the following equation:

$$f_{mnp} = \frac{c}{2\pi\sqrt{\varepsilon_r \mu_r}} \sqrt{\left(\frac{p_{nm}}{R}\right)^2 + \left(\frac{p\pi}{h}\right)^2}, \quad (5)$$

where c is the speed of light in free space, ε_r is the filling material's permittivity, μ_r is the relative permeability, R is the radius of SIW cavity, p_{nm} is the corresponding Bessel function root, m, n, p are the number of variations in standing wave pattern and h refers the thickness of the substrate.

The ANN architecture uses the basic information to fine tune the antenna pattern and dimensions iteratively. By this way, in NDCAANN work, a SIW cavity resonator coaxial antenna is introduced to support 10.84 GHz and 14.82 GHz center resonant frequencies with 15 dB and 30 dB return losses.

In general, antenna prototyping and characteristics analysis is performed manually with the help of some microwave structure analysis software. The input antenna pattern is modified manually based on the simulated or observed results. Changing the antenna pattern in micro-meter precision repeatedly is a tedious process if performed manually. In this proposed method, we introduced an interface to automate the antenna design calibration process which can load a principle antenna

pattern, simulate the characteristics by calling corresponding analytical software and to make changes to the principle base pattern with the help of Artificial Neural Network (ANN). Contribution of Automatic Frequency Characteristics Analyzer, ANN based Fractal Pattern Generator and Nitinol based Pattern selector is the innovation of this proposed method.

IV. PROPOSED METHOD

A Dual band Reconfigurable Fractal Antenna for Wearable Devices (DRFA) work consists of three major modules, they are Automated Frequency Characteristics Analyzer, Artificial Neural Network based Fractal Pattern Generator and Nitinol based Pattern Selector. Same fractal base pattern is used to create different iterative fractal patterns with different dimensions to achieve higher gain for multiband support with higher gain values. The shape memory and super elasticity properties of the Nitinol is used as the key for the reconfigurability of this proposed antenna.

A. Automatic Frequency Characteristics Analyzer (AFCA)

In general, the frequency characteristics of an antenna is observed in a well-equipped laboratory before voluminous manufacturing. Measuring the antenna pattern in a laboratory is a costlier process. Therefore, the researchers and industrial people are using software widely before proceeding with the prototyping of the antenna patterns. These software enables the cost-effective primary characteristics analysis of the antenna patterns.

This kind of software operate on the basis of manual processes such as selecting substrates, feed types, channel guides, sub-band filters, waveguides and dielectric resonators. The patterns are to be drawn manually by the user in the software to get a clear analysis report. Some software possesses the provision of importing images from other compatible applications. If the loaded pattern needs any modifications, then it has to be edited in the software itself to get updated results. Drawing an antenna pattern is a time-consuming process if done manually. AFCA provides a way to automate this process. Ansys HFSS software is used here to analyze the frequency characteristics of the antenna pattern. A dedicated user interface and a service is coded in VC++ to associate with HFSS to feed the vector pattern automatically and retrieve the results from it. AFCA is used as an agent between the user and the HFSS software to reduce repetitive manual processes and to reduce tremendous amount of time.

B. Artificial Neural Network based Fractal Pattern Generator (AFPG)

ANN based fractal pattern generator is designed with the microstrip patch antenna basics and fractal pattern generation. Let L be the length of the microstrip patch antenna, then the fundamental dimension restriction is $L < \frac{\lambda_g}{2}$ where λ_g is the substrate guide wavelength. A basic microstrip patch antenna is illustrated in Fig. 2.

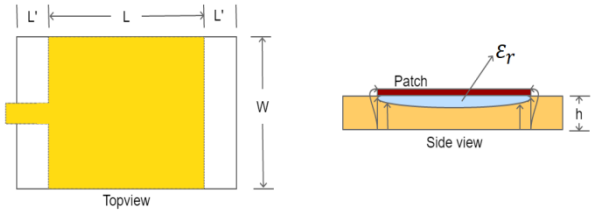

Fig. 2. Microstrip patch antenna.

There are two key points are to be considered while designing a microstrip patch antenna. They are:

- Better efficiency antennas can be designed using thicker substrates and lesser dielectric constants. But the larger element size is high-priced.
- Thin substrate with high dielectric constants will entail tiny element sizes and minimized coupling, but the toll is taken from the efficiency and bandwidths.

Holding these points in consideration, the width w, fringing length correction $\frac{L'}{h}$, patch length L, effective dielectric constant ϵ_{reff}, and feed position z_i are calculated by the following equations for the condition $w \neq \lambda_0$:

$$w = \frac{1}{2f_r\sqrt{\mu_0\epsilon_0}}\sqrt{\frac{2}{\epsilon_r+1}} = \frac{v_0}{2f_r}\sqrt{\frac{2}{\epsilon_r+1}}, \tag{6}$$

$$\frac{L'}{h} = 0.412 \times \frac{(\epsilon_{reff}+0.3)\left(\frac{w}{h}+0.264\right)}{(\epsilon_{reff}+0.258)\left(\frac{w}{h}+0.8\right)}, \tag{7}$$

$$L = \frac{1}{2f_r\sqrt{\epsilon_{reff}}\sqrt{\mu_0\epsilon_0}} - 2L', \tag{8}$$

$$\epsilon_{reff} = \frac{\epsilon_r+1}{2} + \frac{\epsilon_r-1}{2} \times \sqrt{1+\frac{12h}{w}}, \tag{9}$$

$$z_i = \frac{1}{2k}, \tag{10}$$

where,

$$k = \begin{cases} \frac{1}{90}\left(\frac{w}{\lambda_0}\right)^2 if w < \lambda_o \\ \frac{1}{120}\left(\frac{w}{\lambda_0}\right)^2 if w > \lambda_o \end{cases}. \tag{11}$$

The Fractal pattern generation relies on the fractal geometry – which is also known as nature's geometry. The fractal geometry contains chaotic rules with specific interspace rules. Self-similarity at same and different scales, random repetitions, time series scaling or repetitions, detailed small-scale structure and local or global irregularities are the customary characteristics of fractal patterns. The fractal patterns can be generated by some techniques such as Stochastic or deterministic fixed geometry replacement rules, iteration of a map, replicating branching patterns with or without transformations, recurrent relation special time fractals,

random fractals and finite subdivision rules. Iterated Function System (IFS) is used in AFGP module.

Let F_i be the n number of two-dimensional IFS functions and S be the solution set. The Hutchinson's recursive equation states that:

$$S = \bigcup_{i=0}^{n-1} F_i(s). \quad (12)$$

Based on the Barnsley implementation of Equation 12, the two-dimensional function F_i can be represented as a 2×3 matrix that contains Rotation, Scaling, Translation, horizontal flip, vertical flip, incremental 45° flip and shear transformations as follows:

$$F_i(x, y) = (a_i x + b_i y + e_i, c_i x + d_i y + f_i). \quad (13)$$

The first phase of AFPG module is to extract the essential elements from the base antenna pattern. A triangular shape and a rectangular shape as in Fig. 3 are given as the base patterns to the AFPG. The rectangular shape is limited to use with the patch and waveguide where are the triangular shape is set free to construct the fractal pattern.

Fig. 3. Triangle and rectangle base patterns.

Let η be the expected number of central resonant frequencies,Γ be the expected central resonant frequency and ω be the expected bandwidth. Then $\forall i = 1 \rightarrow \eta: (\Gamma_i, \omega_i)$ are the inputs given to the AFPG pattern generation algorithm. Since the pattern generation algorithm has the freedom to generate multiple number of iterations based on Equation (13), getting the fine-tuned dimension vectors the antenna pattern is possible altogether.

The AFPG pattern generation algorithm is given below.

Algorithm 1: AFPG pattern Generation <Input: $(\Gamma_i, \omega_i)[\eta]$, Output: Vector Image>

Step 1: Interpret and load base patterns

Step 2: Estimate and assign dimensions based on equations 6 to 11

Step 3: Call AFCA module

Step 4: Observe generated pattern's frequency characteristics

Step 5: Check observed results with $\forall i = 1 \rightarrow \eta: (\Gamma_i, \omega_i)$ *and go to step 9 if match found*

Step 6: Scale pattern to next size

Step 7: If size exceeds maximum permitted dimension
Resize pattern
Apply pattern generation function by Equation 13

Step 8: Go to step 3

Step 9: Halt process and load converged result to memory

The output of this AFPG algorithm is a vector image that epitomizes the fractal antenna pattern. The amalgamated flow of AFCA and AFPG is given in Fig. 4.

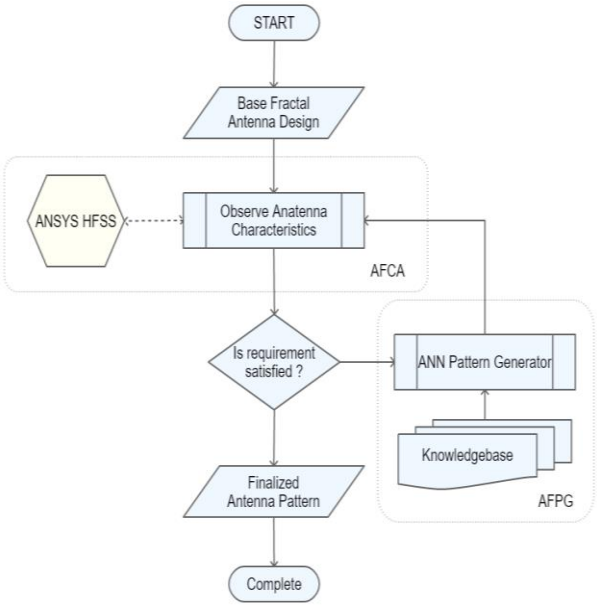

Fig. 4. AFCA and AFPG combined flow diagram.

C. Nitinol based pattern selector

Microstrip patch antennas cannot afford heavy electromagnetic switching arrangements. Therefore, a lightweight switching arrangement is required to alter the connectivity pathways for reconfigurability. Nickel Titanium – which is often represented as Nitinol has the property of shape memory, which is a boon for designing different pathways in microstrip patch antenna. Different pathways of an antenna make it reconfigurable and enables the multiband support attribute. A Nitinol strip is made up of three main substances. The first one is the nitinol substrate which is placed over an elastic steel surface with Kapton insulation [20] material between them. The side view of a typical nitinol switching arrangement is given in Fig. 5.

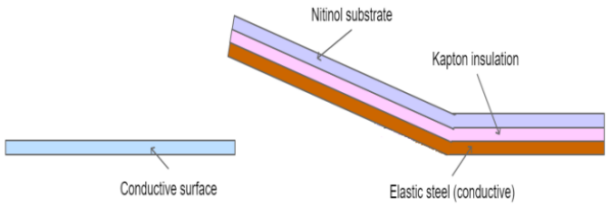

Fig. 5. Nitinol switching arrangement.

The shape of the Nitinol can be controlled using resistive heating methodology. The interesting fact about nitinol is many of the materials get enlarge during the heating process whereas the Nitinol gets shrunk by heating. Since it works as a resistor, it gets some heat naturally while conducting the current and it can be restored to normal position when the heat is reduced by removing current through it. The elastic steel, Kapton insulation and the Nitinol substrate altogether forms the Nitinol strip. The elastic steel is used as the contact, the nitinol substrate us used as the actuator and the Kapton insulation functions as the shape memory by reducing the recovery speed of Nitinol.

This nitinol switching arrangement is used as the antenna pattern selector based on the required bandwidth of proposed dual-band reconfigurable fractal antenna.

V. EXPERIMENTAL SETUP

A high-power computer is required to get the converged result of ANN since the AFPG module overstepped thousands of iterations. HFSS software is also a fairly high computational resource demanding one. Therefore, the experimental setup is split into two different computational environments. A dedicated cloud server with Xeon E5-2620v4 12 core processor equipped with 16GB DDR4 2400MHz RAM is leased to execute the AFPG and AFCA modules. A laptop with Intel Core i5 processor and 4GB RAM is used as the remote loader and monitor for the AFPG and AFCA modules. A dedicated UI is used to initialize, execute and monitor the proposed method in the server. The server will continue to run and log the converged antenna patterns even after shutting down the remote-control laptop. The UI will fetch the most recent converged pattern whenever it is getting executed in the remote laptop. Experimental setup architecture is given in Fig. 6.

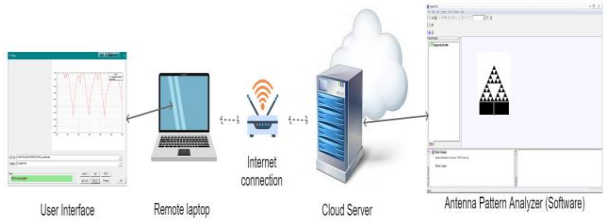

Fig. 6. Experimental setup.

VI. RESULTS AND ANALYSIS

The converged ANN antenna pattern based on the elementary based patterns as in Fig. 3 at 211602nd iteration is given below in Fig. 7 (a) and Nitinol Strip switching placements are given in Fig. 7 (b).

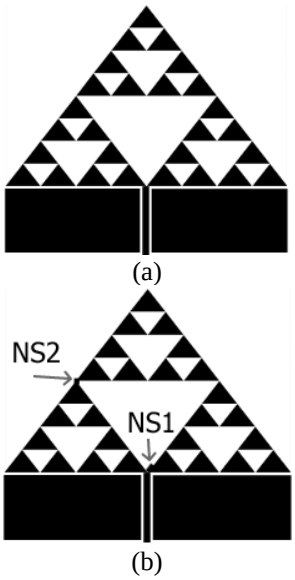

Fig. 7. (a) Converged antenna pattern, and (b) Nitinol switch placement.

NS1 and NS2 in Fig. 7 (b) are the first and second nitinol switch placements. The switching configurations can be set to four possible cases as in Table 1.

Table 1: Switching status and selected modes

NS1	NS2	Configuration
Off	Off	Mode 0
Off	On	Mode 1
On	Off	Mode 2
On	On	Mode 3

Obtained antenna patterns by using NS1 and NS2 in all 4 configuration modes are given in Fig. 8.

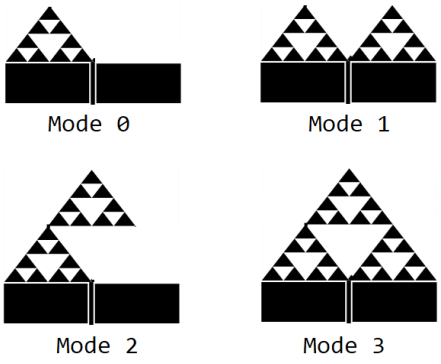

Fig. 8. Mode pattern configuration.

A. Configuration mode 0

Configuration mode 0 is selected when both NS1 and NS2 Nitinol strips are on off state. The resonant frequency characteristics of this configuration are given in Fig. 9.

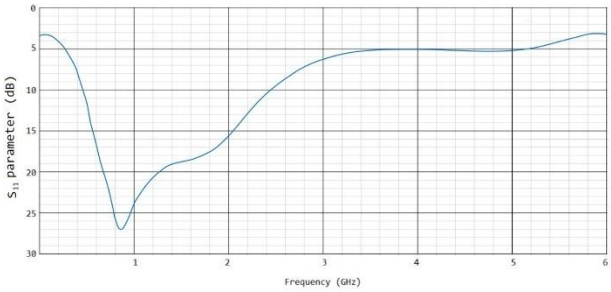

Fig. 9. Return loss graph of configuration mode 0.

Based on the observations, mode 0 reached less than 25 dB between 800MHz and 950 MHz which comes under GSM bandwidth. The gain is about 6 ~ 7.2 dB in the resonant frequency band. This mode does not get enough gain for 2.4 GHz which reveals that mode 0 is not suitable for Bluetooth or Wi-Fi communication.

B. Configuration mode 1

Configuration mode 1 is achieved while NS1 is on position and NS2 is in off position. This mode supports two different frequency bands of 850 MHz ~ 1.05 GHz and 2 GHz ~ 2.6 GHz which is suitable for GSM, Bluetooth and Wi-Fi applications. The peak gain 7.7 dB is achieved in 2.38 GHz resonance frequency as shown in Fig. 10.

C. Configuration mode 2

This configuration mode is achieved by turning off NS1 and turning on NS2. This mode also supports two different resonant frequency bands with 2.4 GHz and 5.18 GHz center frequency. The 2.4 GHz band ranges from 2.2 GHz to 2.76 GHz and the 5.18 GHz band ranges from 4.96 GHz to 5.38 GHz with lesser then 25 dB of return loss. The simulation graph is given in Fig. 11.

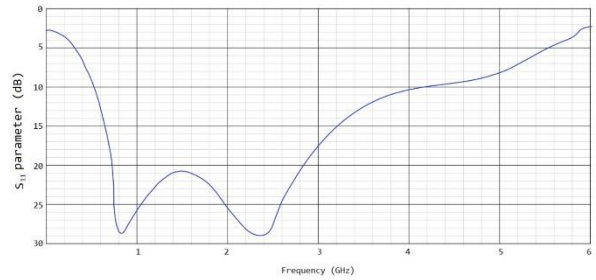

Fig. 10. Return loss graph of configuration mode 1.

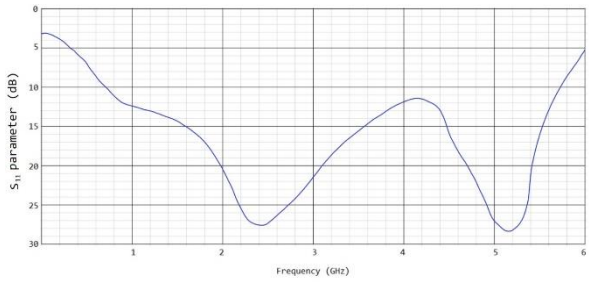

Fig. 11. Configuration mode 2 return loss graph.

Configuration mode 2 can be used for Bluetooth and Wi-Fi applications with its 7.7 dB gain at 2.4 GHz. The gain of 8.2 dB at 5.18 GHz makes it possible to use for 5G applications.

D. Configuration mode 3

This pattern configuration is accomplished by turning on both NS1 and NS2 Nitinol switching arrangements. Three frequency band widths with 700 MHz, 2.38 GHz and 5.1 GHz center frequencies are achieved in this configuration. The obtained bandwidths are 580 MHz ~ 1.1 GHz, 2.18 GHz ~ 2.6 GHz and 4.82 GHz ~ 5.23 GHz with less than 25 dB return loss. This mode is suitable for GSM, Bluetooth, Wi-Fi and 5G applications.

The gain at 700 MHz, 2.38 GHz and 5.1 GHz center frequencies are about 8.2 dB, 6 dB and 6.2 dB. The Power Standing Wave Ratio (PSWR) for the generated antenna pattern is 1.21 as measured in the simulation. The return loss graph of configuration mode 3 is given in Fig. 12 and the comparison of return loss, gain and VSWR for various frequency are given in Table 2.

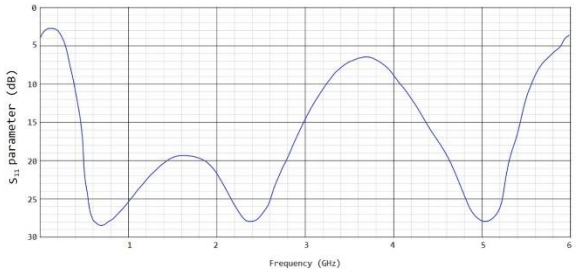

Fig. 12. Configuration mode 3 return loss graph.

The antenna has fabricated for our proposed method and also the radiation pattern of configuration mode 3 is given in the Fig. 13. The measured values of Return loss (RL), Gain and Voltage Standing Wave Ratio (VSWR) are listed in the Table 2.

Figure 14 shows the S11 parameter values by comparing the measured and simulated data for different frequencies.

Table 2: RL-Gain-VSWR graph

Frequency (GHz)	Return Loss (dB)	Gain (dB)	VSWR (dB)
0.5	4.8	-22	3.71
0.7	28.5	27	1.07
1	25.4	21	1.11
1.5	19.5	9	1.23
2	23.5	13.8	1.14
2.28	28	26	1.08
2.5	27	22	1.09
3	14.5	-1	1.46
3.5	7	-16	2.61
4	8.9	-12.1	2.11
4.5	17.5	5	1.31
5	27.9	25.7	1.09
5.5	12.4	-6.99	1.63
6	3.7	-22.8	4.76

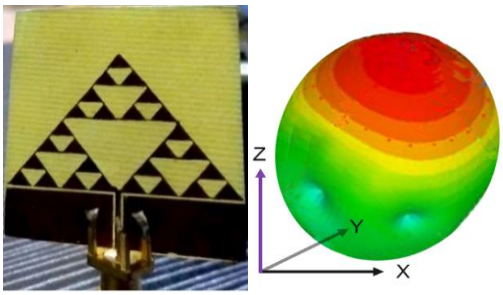

Fig. 13. Fabricated antenna and mode 3 radiation pattern.

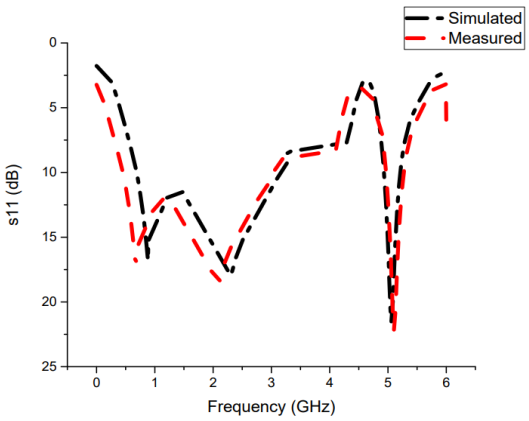

Fig. 14. S11 parameter measured vs simulated graph.

VII. CONCLUSION

A fractal image inspired antenna pattern is achieved with the help of ANN and the proposed reconfigurable antenna comprehends GSM, Bluetooth, Wi-Fi and 5G bands which is very suitable for wearable devices such as health wristbands. The reconfigurable property is achieved by presenting Nitinol based micro switching mechanism. The configuration mode 0 supports only GSM band with lesser bandwidth which has the less scope of applications. But Configuration mode 1 and 2 are supporting GSM + Wi-Fi applications and Wi-Fi + 5G applications respectively. Configuration mode 3 supports GSM, Bluetooth, Wi-Fi and 5G frequency bands with acceptable gain values. Many of the upcoming digital gadgets are having the communication capability in GSM, Wi-Fi and 5G bands. A wearable microstrip antenna that supports these bands will be very helpful for personal care electronic gadgets and wearable devices. Hence, the proposed antenna pattern may be recommended for the impending wearable electronic communication devices.

REFERENCES

[1] A. Shehab, A. Ismail, L. Osman, M. Elhoseny, and I. M. El-Henawy, "Quantified self using iot wearable devices," *Proceedings of the International Conference on Advanced Intelligent Systems and Informatics*, Springer, pp. 820-831, 2017.

[2] A. Y. I. Ashyap, Z. Z. Abidin, S. H. Dahlan, H. A. Majid, M. R. Kamarudin, and R. A. Abd-Alhameed, "Robust low-profile electromagnetic band-gap-based on textile wearable antennas for medical application," *International Workshop on Antenna Technology: Small Antennas, Innovative Structures, and Applications (iWAT)*, Athens, pp. 158-161, 2017.

[3] L. Wen, S. Gao, Q. Luo, Q. Yang, W. Hu, and Y. Yin, "A low-cost differentially driven dual-polarized patch antenna by using open-loop resonators," in *IEEE Transactions on Antennas and Propagation*, vol. 67, no. 4, pp. 2745-2750, Apr. 2019.

[4] M. Tang, X. Chen, M. Li, and R. W. Ziolkowski, "A bandwidth-enhanced, compact, single-feed, low-profile, multilayered, circularly polarized patch antenna," in *IEEE Antennas and Wireless Propagation Letters*, vol. 16, pp. 2258-2261, 2017.

[5] Y. Cai, K. Li, Y. Yin, S. Gao, W. Hu, and L. Zhao, "A low-profile frequency reconfigurable grid-slotted patch antenna," in *IEEE Access*, vol. 6, pp. 36305-36312, 2018.

[6] R. L. Haupt, "Optimizing the sidelobe level of a two-way antenna array pattern by thinning the receive aperture," 2018 *International Conference on Radar (RADAR)*, Brisbane, QLD, pp. 1-5, 2018.

[7] H. Li, Y. Jiang, Y. Ding, J. Tan, and J. Zhou, "Low-sidelobe pattern synthesis for sparse conformal arrays based on PSO-SOCP optimization," in *IEEE Access*, vol. 6, pp. 77429-77439, 2018.

[8] N. Gupta, J. Saxena, and K. S. Bhatia, "Optimized metamaterial-loaded fractal antenna using modified hybrid BF-PSO algorithm," in *Neural Computing and Applications*, Springer, pp. 1-18, 2019.

[9] R. N. Biswas, A. Saha, S. K. Mitra, and M. K. Naskar, "PSO-based antenna pattern synthesis: A

paradigm for secured data communications," in *Nature-Inspired Algorithms for Big Data Frameworks - IGI Global Disseminator of Knowledge, IGI-Global*, pp. 1-28, 2019.

[10] S. Bhatt, P. Mankodi, A. Desai, and R. Patel, "Analysis of ultra-wideband fractal antenna designs and their applications for wireless communication: A survey," *2017 International Conference on Inventive Systems and Control (ICISC)*, Coimbatore, pp. 1-6, 2017.

[11] N. K. Darimireddy, R. R. Reddy, and A. M. Prasad, "A miniaturized hexagonal-triangular fractal antenna for wide-band applications [Antenna Applications Corner]," in *IEEE Antennas and Propagation Magazine*, vol. 60, no. 2, pp. 104-110, Apr. 2018.

[12] Md. M. Hasan, M. R. I. Faruque, and M. T. Islam, "Dual band metamaterial antenna for LTE/Bluetooth/WiMAX system," in *Scientific Reports*, Springer, vol. 8, no. 1240, pp. 1-17, 2018.

[13] C. Mao, S. Gao, Y. Wang, Y. Liu, X. Yang, Z. Cheng, and Y. Geng, "Integrated dual-band filtering/duplexing antennas," in *IEEE Access*, vol. 6, pp. 8403-8411, 2018.

[14] Z. Zhao, J. Lai, B. Feng, and C. Sim, "A dual-polarized dual-band antenna with high gain for 2G/3G/LTE indoor communications," in *IEEE Access*, vol. 6, pp. 61623-61632, 2018.

[15] S. Gao, L. Ge, D. Zhang, and W. Qin, "Low-profile dual-band stacked microstrip monopolar patch antenna for WLAN and car-to-car communications," in *IEEE Access*, vol. 6, pp. 69575-69581, 2018.

[16] M. Elhabchi, M. N. Srifi, and R. Touahni, "A novel dual band hexagonal antenna for bluetooth and UWB applications with single band notched," in *Advanced Electromagnetics Journal*, vol. 7, no. 5, pp. 63-68, 2018.

[17] J. Zhang and Z. Shen, "Dual-band shared-aperture UHF/UWB RFID reader antenna of circular polarization," in *IEEE Transactions on Antennas and Propagation*, vol. 66, no. 8, pp. 3886-3893, Aug. 2018.

[18] N. K. Darimireddy, R. R. Reddy, and A. M. Prasad, "A miniaturized hexagonal-triangular fractal antenna for wide-band applications [Antenna Applications Corner]," in *IEEE Antennas and Propagation Magazine*, vol. 60, no. 2, pp. 104-110, Apr. 2018.

[19] M. Chetioui, A. Boudkhil, N. Benabdallah, and N. Benahmed, "A novel dualband coaxial-fed SIW cavity resonator antenna using ANN modeling," in *Journal of Engineering Science and Technology*, review 11, article 2, pp. 82-87, JESTR, 2018.

[20] E. E. Shin, D. A. Scheiman, and M. Lizcano, "Lightweight, durable, and multifunctional electrical insulation material systems for high voltage applications," 2018 *AIAA/IEEE Electric Aircraft Technologies Symposium (EATS)*, Cincinnati, OH, pp. 1-21, 2018.

A. Sivabalan working as an Assistant Professor in Chennai Institute of Technology. Received the B.E. degree in Electronics and Communication Engineering from Dhanalakshmi College of Engineering, Chennai Anna University, India, in 2009, received M.E. degree in Communication Systems from Sri Sairam Engineering College, Chennai, Anna University, Chennai, India, in 2012. Currently pursuing Ph.D. in "Design of reconfigurable antenna for medical applications". He had published two international Journals.

P. Jothilakshmi working as a Professor in the Department of Electronics and Communication Engineering, Sri Venkateswara College of Engineering, Chennai. Her research area is Microwave Antennas - Design and Analysis of a Class of Continuous Transverse Stub Array Antenna for Microwave Applications Anna University - Chennai-2015, M.E. (Communication Systems) – Mepco Schlenk Engineering College, Sivakasi- December 2000, B.E. (Electronics and Communication Engineering) – Thanthai Periyar Government Institute of Technology. She has published more than 100 research papers in international and national journals including IEEE conferences and SCI Indexed journals.